Wavelet-Based Adaptive Anisotropic Diffusion Filter

Ufuk TANYERI[1], Recep DEMIRCI[2]
[1]*Department of Computer Technologies, Ankara University, Ankara, 06920, Turkey*
[2]*Department of Computer Engineering, Gazi University, Ankara, 06500, Turkey*
ufuktanyeri@ankara.edu.tr

***Abstract*—Its multiplicative nature complicates speckle noise reduction in images because of the effort required for separation of noisy pixels from other pixels. In this study, a novel adaptive anisotropic diffusion filter algorithm based on Haar wavelet transform has been proposed. Initially, Haar transform of image to be filtered was taken and then median absolute deviation of wavelet coefficients was used to tune the conductance parameter, *K* of diffusion filter with different diffusion functions. The suggested strategy has been tested with different images and different noise variances. Moreover, experimental results have been compared with conventional diffusion filters, and also Lee filter and Wiener filter which are frequently used for despeckling.**

***Index Terms*—image denoising, discrete wavelet transforms, anisotropic, adaptive filters, nonlinear filters.**

I. INTRODUCTION

Noises in images have either additive or multiplicative characteristics. Speckle noise is a multiplicative noise and indicates an undesirable random signal attained during capturing and transferring signal [1]. Images with this kind of signals are called the corrupted images. It is important to reduce the effect of noise in image processing applications such as segmentation and recognition so that the accurate results could be obtained. Since speckle noise has a grainy structure in image, more effort than that of filtering of other noises is required for despeckling [2-3]. In this sense, many speckle noise reduction algorithms have been developed up to date. Perona and Malik proposed nonlinear heat diffusion algorithm for noise reduction in 1990 [4], but the requirement of user-defined parameters was the main drawback of the method. Authors in reference [5] and reference [6] modified primitive diffusivity functions suggested by Perona and Malik, and recommended new diffusivity functions. Black et al. considered Tukey's biweight scheme for a statistical solution to diffusivity problem [7]. Despite varieties of improvements, the speckle noise removal capabilities of conventional nonlinear diffusion filter have been insufficient since proper conductance parameters of filters for images with different noise variances must be determined by the user [3]. Consequently, user dependency and value of conductance parameter *K* are main issues with conventional nonlinear diffusion as shown in Fig. 1.

Additionally, it was shown by researchers that although anisotropic diffusion filter was successful for additive noise, it was not good enough for image degraded speckle noise [8]. Edge preserving capacities of image filter are essential as much as filtering performances.

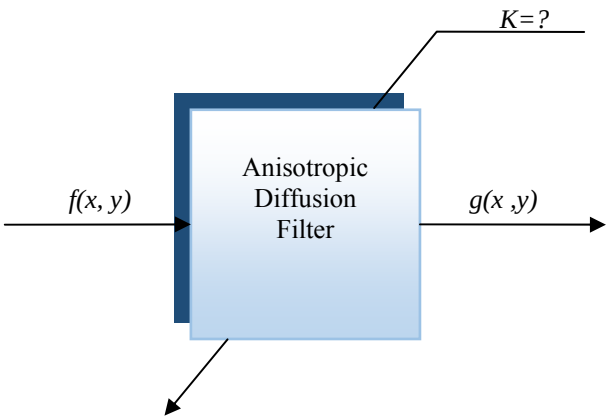

Figure 1. Problem with a conventional nonlinear diffusion filter

In 2001, Aja et al. presented that linear and median filters didn't preserve edge of images degraded with speckle noise [9]. Although many approaches have been proposed for a solution, most of them suffer from computation costs. In 2004, Gupta et al. suggested a filtering strategy using logarithmic transformation; multiscale decomposition and variance of wavelet transform results [10]. But, the cost of the implementation was so high. Accordingly, adaptive methods to overcome the user dependency and computation cost have been indispensable. The other some approaches were to transform multiplicative noise into additional noise through logarithmic computations, too. Then homomorphic filter was employed within transformed images [3, 11-12].

Performance of the adaptive filtering scheme highly depends on conductance parameter *K* and the determination of it is a critical issue [13]. Automatic estimation of conductance parameter *K* for each noise image to be filtered has been the recent research subject in the area of anisotropic image filtering. In 2006, Aja-Fernández et al. suggested to use median and median absolute deviation (MAD) of the image as conductance parameter estimator [14]. Krissian et al. emphasized the importance of accurate estimator with stable iterations [15]. Some approaches to noise estimation emphasized the importance of mathematical approaches rather than statistical approaches [16-17]. Kbiri Alaoui et al. proved that the diffusion filter would be solved using the space of functions [18]. Nevertheless, conductance parameter, *K* and stopping criteria still depend on user intervention.

In this study, a novel adaptive speckle noise reduction algorithm using anisotropic diffusion filter based on Haar wavelet transform and the median absolute deviation was proposed. In offered strategy, no user intervention is

Digital Object Identifier 10.4316/AECE.2018.04012

required. It is noticed that the proposed method not only preserves edges but also filters speckles in the image.

II. Anisotropic Diffusion Filter

As mentioned in the introduction section, many filters have been developed by researchers for reducing noise in the degraded image. Their main aims were to obtain better-preserved edge and fine-scale details in the image while filtering. One of the filters used for this purpose is called a nonlinear diffusion filter proposed by Perona and Malik in 1990 [4]. The anisotropic diffusion filter was based on heat equations as follows:

$$\frac{\partial I(x,y;t)}{\partial t} = div(c(x,y;t)\,\nabla I(x,y;t)) \qquad I(x,y;0) = I_0(x,y) \tag{1}$$

where *div* is divergence and ∇ is the gradient operator. The *c* is conductance or diffusivity function and it must be close to 1 in each region and 0 at the edge of the image, *I(x,y)*. $I_0(x,y)$ represents the image degraded with speckle noisy at the time *t=0*. So far, several diffusivity functions have been developed by many researchers since it is vital for the filtering process. Commonly used diffusion functions, *c* in (1) were recommended by Perona and Malik (PM) [4], Charbonnier et al. (CH) [5], and Weickert (WC) [6] as follows:

$$c(x,y,t) = 1 \Big/ 1 + \left(\|\nabla I\| / K \right)^2 \tag{2}$$

$$c(x,y,t) = 1 \Big/ \sqrt{1 + \left(\|\nabla I\| / K \right)^2} \tag{3}$$

$$c(x,y,t) = \begin{cases} 1 & \|\nabla I\| = 0 \\ 1 - \exp\left(\dfrac{-2.33666}{\left(\|\nabla I\| / K \right)^4} \right) & \|\nabla I\| > 0 \end{cases} \tag{4}$$

where *K* is the most crucial parameter determined by the user according to the image, and it should be appropriately selected for every noisy image.

III. Haar Wavelet Transform

Haar wavelet transform is a kind of discrete wavelet transform. This transformation detects the high and low-frequency components of the image. It is a vital part of the proposed method because of its separating capability of noisy pixels in the image [12]. Haar wavelet transform is defined as:

$$f(x) = c_0 + \sum_{j=0}^{\infty} \sum_{k=0}^{2^j - 1} c_{jk} \psi_{jk}(x) \tag{5}$$

where *j* is non-negative integer scale factor, *k* is translation parameter $0 \le k \le 2^j - 1$, and c_{jk} is scale function. On the other hand, ψ_{jk} is a function derived from mother function of wavelets, which is represented by $\psi_{jk}(x) = \psi\left(2^j x - k\right)$. Main wavelet function is defined as

$$\psi(x) = \begin{cases} 1 & 0 \le x < \dfrac{1}{2}, \\ -1 & \dfrac{1}{2} < x \le 1, \\ 0 & otherwise. \end{cases} \tag{6}$$

Pixels belong to noise and edge in the image are located at high-frequency components of wavelet: horizontal, vertical, and diagonal coefficients. Subsequently, noisy pixels in the image are easily detected utilizing these coefficients. The well-known Cameraman is shown in Fig. 2(a) was degraded with speckle noise as shown in Fig. 2(b). The Haar wavelet coefficients of the original image in horizontal, vertical, and diagonal directions were shown in Fig. 3(a), Fig. 3(b), and Fig. 3(c), respectively. Also, Haar wavelet coefficients of degraded Cameraman image in horizontal, vertical, and diagonal directions were shown in Fig. 3(d), Fig. 3(e), and Fig. 3(f), respectively. When it is carefully looked at, it is possible to see the effect of noise in Haar wavelet coefficients. Also, histograms of horizontal, vertical, and diagonal images were also obtained in Fig. 4(a), Fig. 4(b), and Fig. 4(c), respectively. Typically, the normalized histogram with the total number of pixels is used as a pre-processing in image processing applications such as image retrieval, segmentation and filtering [19-21]. As could be seen in Fig. 4, the histogram curves of noisy images are shifted to the right relative to the original image.

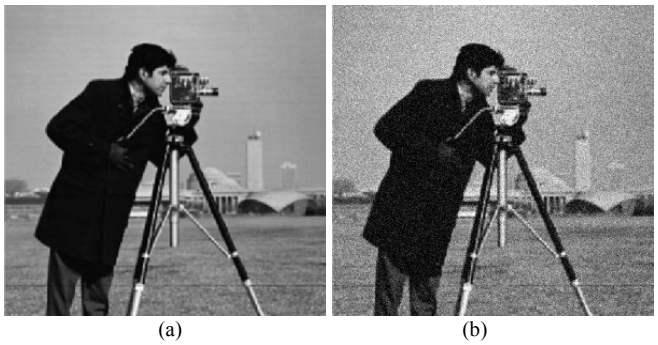

(a) (b)

Figure 2. Cameraman a) Original b) Degraded with speckle noise (σ=0.01, PSNR= 23.15 dB)

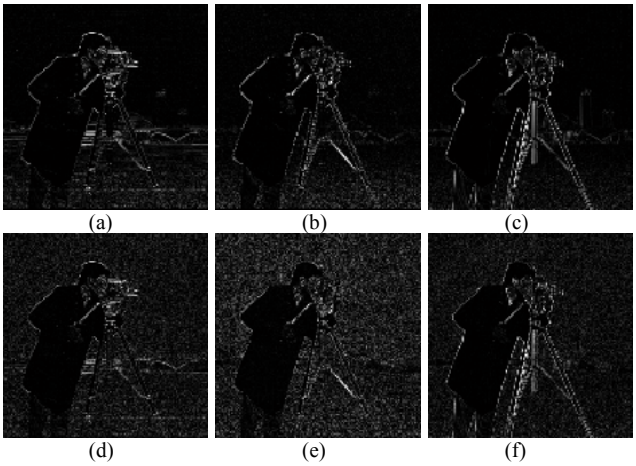

(a) (b) (c)

(d) (e) (f)

Figure 3. Haar wavelet coefficients of original a) horizontal b) vertical c) diagonal, and of noisy images d) horizontal e) vertical f) diagonal

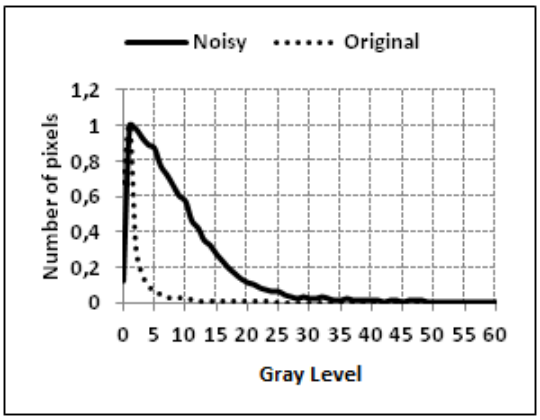

(a)

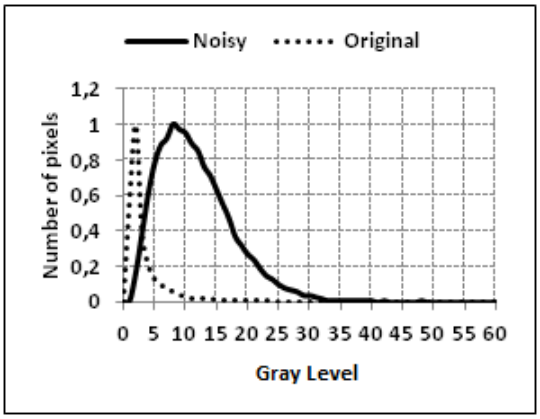

(b)

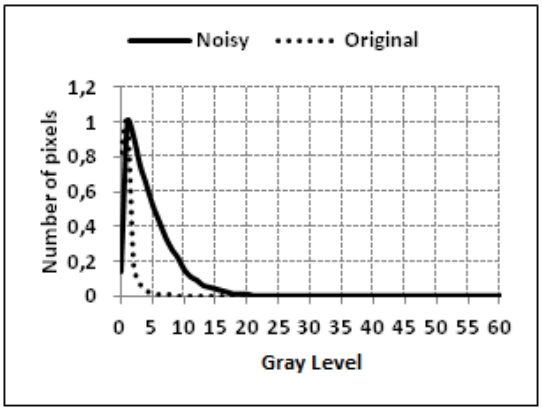

(c)

Figure 4. Normalized histograms of wavelet coefficients of Cameraman a) horizontal b) vertical c) diagonal

This means that the wavelet transform of image holds significant information about the presence of noise. The problem is to convert the related information into a single value. If it could be done somehow, the original image and noisy image will have different values. Consequently, noise information from histograms could be reduced as a single parameter. Mercorelli and Frick used Haar wavelet transform as useful noise estimator [22]. Then it was employed in the anisotropic diffusion filter, and Finn et al. observed that even though anisotropic diffusion filter based on wavelet transform was successful regarding the reduction of speckle noise, it failed to adequately prevent the edges in the image [23]. Furthermore, the center of gravity of the histogram of the wavelet transform was employed as noise estimator by authors [24]. In this study, the anisotropic diffusion filter has been performed by the estimated values, and it has been compared with conventional diffusion filter and well-known Lee and Wiener filter to demonstrate the superiority of the method.

Apart from noise estimator using wavelet transform, image filtering could be done by thresholding wavelet coefficients. In VisuShrink approach, the diagonal coefficient of wavelet transform was used for thresholding [25] whereas the wavelet coefficients in each direction were separately used in SureShrink [26], and BayesShrink methods [27]. Although wavelet shrinking methods produce smoothed images, they are profoundly affected by the dimension of images, and edge persevering capabilities are weak [28]. The wavelet transform in the literature appears to be frequently used in this context [29].

IV. Adaptive Anisotropic Diffusion Filter

The numerical implementation of (1) was done to achieve anisotropic diffusion filter as follows:

$$I_{i,j}^{t+1} = I_{i,j}^{t} + \lambda\left[c_N \nabla_N I + c_S \nabla_S I + c_E \nabla_E I + c_W \nabla_W I\right]_{i,j}^{t} \quad (7)$$

where i and j are spatial coordinates of pixels, c is diffusivity coefficient in each direction, N, S, E, W are the mnemonic subscripts for North, South, East, and West, λ is chosen for the stable scheme, which is $[0,1/4]$, and t is iteration time. Accordingly, spatial directions of anisotropic diffusion are shown in Fig. 5.

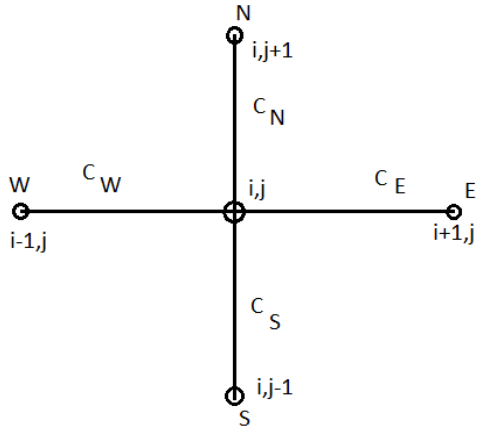

Figure 5. Diffusion directions in the image

Although the anisotropic diffusion filters for images have many advantages over conventional filters, the selection of suitable conduction parameter, K has remained an unsolved issue. In this study, an automatic mechanism to tune K has been developed. Initially, Haar wavelet transform of the noisy image, $I_0(x,y)$ was obtained. Then the median absolute deviations of the coefficient in each direction were computed. The MAD of the image is a robust statistical scheme and was previously used to tune image filter based on the gradient of the noisy image [7]. Also, Sun and Xu used it as noise estimator for image segmentation as well [30]. Although the gradient of the image produces significant information about edge and noises, directional intensity changes were not individually considered in gradient technique. Only magnitude information was used. On the other hand, anisotropic diffusion filter works depending on directions. Therefore, the parameter obtained with gradient magnitude could not be satisfactory. However, the wavelet transform considers directional intensity variations independently. This information obtained from wavelet transformation is quite parallel with anisotropic

diffusion. This was motivation point of suggested adaptive anisotropic diffusion filter. Consequently, the design stages of developed image filter were completed as follows:

Step 1. Calculate Haar wavelet coefficients in horizontal, vertical, and diagonal, $I_{H(x,y)}, I_{V(x,y)}, I_{D(x,y)}$ of the noisy image using (5) and (6).

Step 2. Calculate MAD from the normalized histogram of the each of coefficients as:

$$horizontal\ \ direction;\ K_h = median\left[I_{H(x,y)} - median\left(I_{H(x,y)}\right)\right] \quad (8)$$

$$vertical\ \ direction;\ K_v = median\left[I_{V(x,y)} - median\left(I_{V(x,y)}\right)\right] \quad (9)$$

$$diagonal\ \ direction;\ K_d = median\left[I_{D(x,y)} - median\left(I_{D(x,y)}\right)\right] \quad (10)$$

Step 3. Calculate average of MAD as:

$$K = \frac{K_h + K_v + K_d}{3} \quad (11)$$

Step 4. Substitute the value obtained in step 3 into (2), (3), and (4) for each direction as shown in Fig. 5. The whole structure of the proposed adaptive anisotropic diffusion filter was shown in Fig. 6.

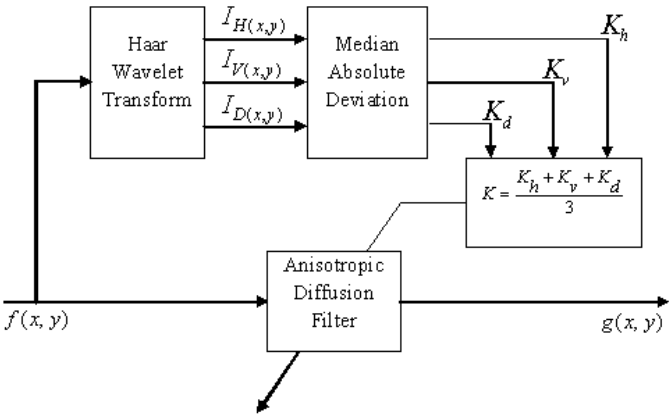

Figure 6. A block diagram of proposed adaptive diffusion filter

V. Performance Criteria

The objective performance comparison of image filters could be done by using the mean square error (MSE), peak signal to noise ratio (PSNR), and the structural similarity (SSIM) index proposed by Wang et al. [31] was used. The MSE is defined as

$$MSE = \frac{1}{M\,N} \sum_{i=0}^{M-1} \sum_{j=0}^{N-1} \left(f(x_i, y_j) - g(x_i, y_j) \right)^2 \quad (12)$$

where *f(x, y)* and *g(x, y)* are the original and the filtered images, respectively. The PSNR is stated as:

$$PSNR = 10 \log_{10} \left(\frac{255^2}{MSE} \right) \quad (13)$$

Additionally, the structural similarity index between two images *f*, *g* is:

$$SSIM(f, g) = \frac{(2\mu_f \mu_g + c_1)(2\sigma_{fg} + c_2)}{(\mu_f^2 + \mu_g^2 + c_1)(\sigma_f^2 + \sigma_g^2 + c_2)} \quad (14)$$

where μ_f and μ_g are means of image *f(x, y)* and *g(x, y)*, respectively. The σ_f and σ_g are variances of image *f(x, y)* and *g(x, y)*, respectively and σ_{fg} is covariance of *f(x, y)* and *g(x, y)*. Parameters: c_1 and c_2 are selected according to the suggestion of Wang et al. [31] as $c_1 = (0.01 * L)^2$ and $c_2 = (0.03 * L)^2$ where *L* is maximum intensity level, 255.

Diffusion filters are iterative filters. Therefore, while employing (12), (13), and (14) for performance comparison, the image *f(x, y)* and *g(x, y)* are replaced by $I_{i,j}^{t}$ and $I_{i,j}^{t+1}$, respectively. Consequently, if image *f(x, y)* and *g(x, y)* are close to each other, the MSE goes to zero whereas the SSIM goes to one.

VI. Experimental Results and Discussions

Experimental verification of the proposed strategy, a well-known Cameraman, synthetic and brain tomography images [32] was corrupted by adding the speckle noise. All of the test images corrupted by speckle noise are filtered using diffusivity functions of Perona Malik, Charbonnier, and Weickert. Since there has not been a definite criterion for selection of conductance parameter, the conventional diffusion filter with the PM diffusivity function with randomly tuned conductance parameter, *K*: 25, 50, and 100 were tested with Cameraman images. Iteration number, *t* was fixed as 50 for all experiments.

Fig. 7(a), Fig. 7(b) and Fig. 7(c) shown filter outputs for *K*: 25, 50 and 100, respectively. It was observed that arbitrarily selected diffusion parameters produced unsatisfactory results as edge information or object boundaries were blurred. Additionally, as Lee [33] and Wiener [34] filters are commonly used for speckle noise reduction [28], [33-35], Lee and Wiener's filters were employed to the denoise image for the reason that speckle noise was added into the original image. Fig. 7(d) and Fig. 7(e) show responses of Lee and Wiener filters, respectively. Since the edges in the image were not adequately protected, their performances are insufficient.

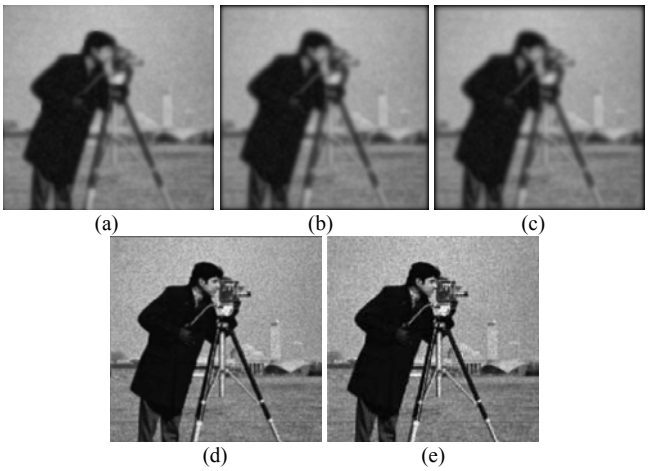

Figure 7. Cameraman a) *K*: 25, SSIM: 0.9480 b) *K*: 50, SSIM: 0.8957 c) *K*: 100, SSIM: 0.8835 d) Lee, SSIM: 0,9851 e) Wiener, SSIM: 0,9884

It can be seen that the conductance parameter, *K* is crucial for degraded images with speckle. In this sense, the conventional diffusion filter by using different values of conductance parameter blurred the edges in the image. This means that it doesn't preserve the edges of the image.

Conventional diffusion filter uses the same conductance parameter, K in the whole image and is user-dependent. It is a drawback for conventional diffusion filter. Adaptive anisotropic diffusion filter recommended was tested for Cameraman image by using different diffusivity functions. Fig. 8(a), Fig. 8(b), and Fig. 8(c) shows the output of the image filter with Perona and Malik, Charbonnier, and Weickert functions, respectively. As could be seen, edge-preserving capacities and the SSIM values are better than that of convention diffusion filters. Additional, variation curves of PSNR versus iteration time for Cameraman were shown in Fig. 9. The experiments were completed with Perona and Malik, Charbonnier, and Weickert functions. Although the success of Weickert functions is insignificant at the beginning, it becomes the best of them as time increases. Therefore, it was concluded that Weickert function was the best choice with our proposal.

The proposed diffusion filter, Lee and Wiener filters were tested with Cameraman image for different noise variances: {0,01, 0,02, 0,04, 0,08, 0,1, 0,12, 0,14, 0,16, 0,28, and 0,20}. The SSIM and PSNR curves obtained with different filters were shown in Fig. 10(a) and Fig. 10(b) respectively where the robustness of developed adaptive filter could be easily seen.

(a)

(b)

(c)

Figure 8. Cameraman with proposed filter with K=(4+4+2)/3 a) PM, PSNR: 29.40 dB, SSIM: 0,9904 b) CH, PSNR: 31.03 dB, SSIM: 0.9933 c) WC, PSNR: 33.29 dB, SSIM: 0.9960

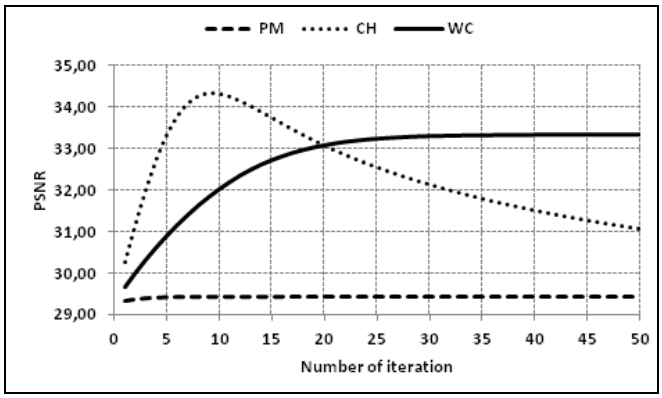

Figure 9. Cameraman: PSNR versus iteration time, t

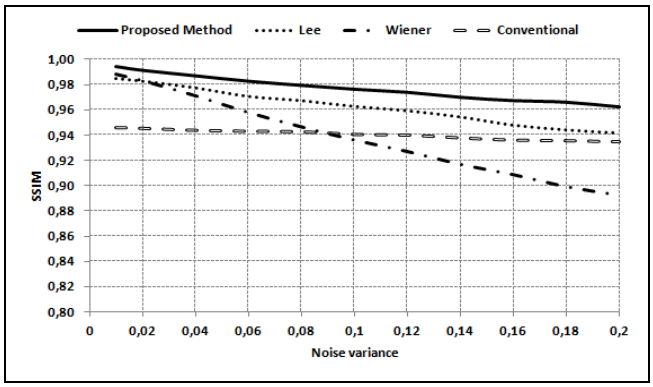

(a)

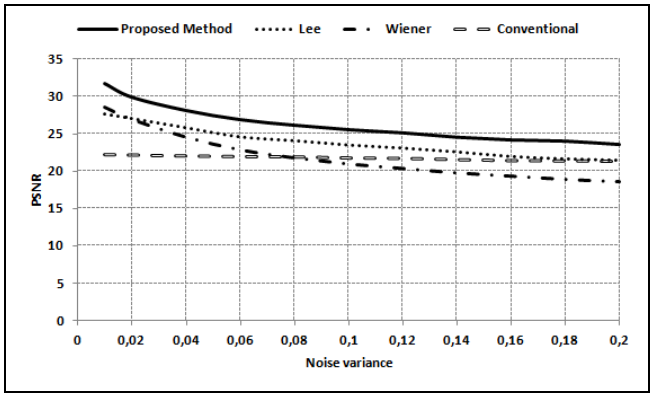

(b)

Figure 10. Performance curves with Cameraman a) SSIM versus variance b) PSNR versus noise variance

Apart from the standard test image, synthetic image shown in Fig. 11(a) and its noisy version shown in Fig. 11(b) were also employed to understand the performance of devised image filter. Although SSIM values of Lee and Wiener filter are high, their visual judgment is not satisfactory as shown in Fig. 11(c) and Fig. 11(d), respectively. On the other hand, the performance of the proposed filter is better than that of conventional diffusion filter as shown in Fig. 11(e) and in Fig. 11(f). Additionally, the robustness of the proposal for the synthetic image was confirmed. The related SSIM and PSNR responses are shown in Fig. 12(a) and in Fig. 12(b), respectively.

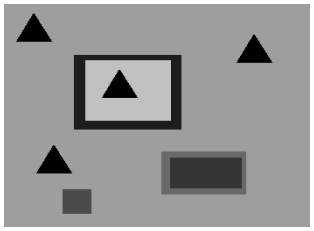

(a)

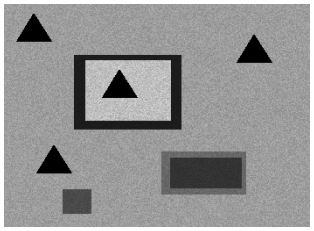

(b)

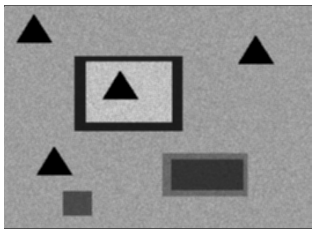

(c)

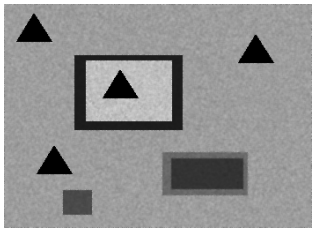

(d)

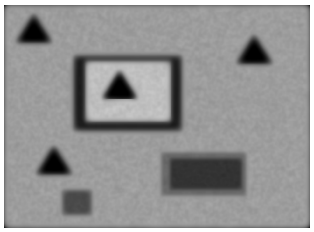

(e)

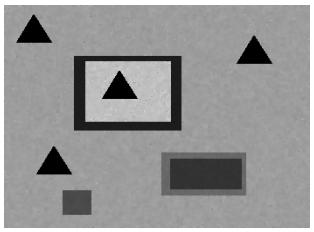

(f)

Figure 11. Synthetic image a) Original b) Degraded with σ=0.01 c) Lee, SSIM: 0.9590 d) Wiener, SSIM: 0.9957 e) Conventional diffusion filter, SSIM: 0.9243 f) Proposed filter, SSIM: 0.9977

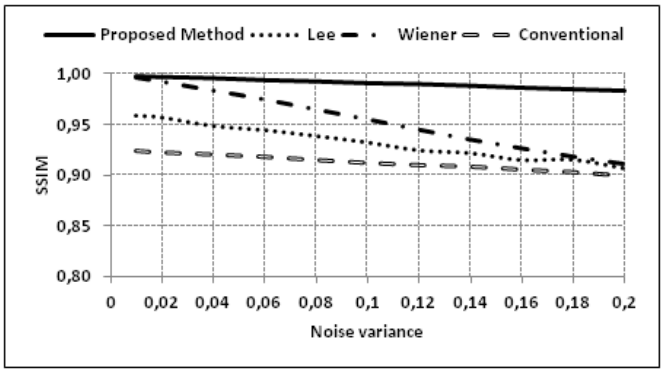

(a)

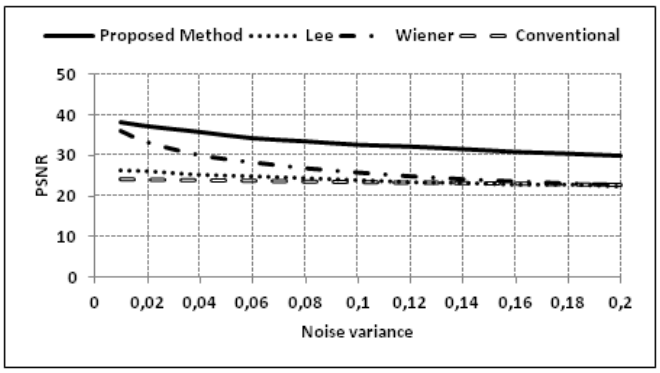

(b)

Figure 12. Performance curves with synthetic a) SSIM versus variance b) PSNR versus noise variance

Figure 13. Brain tomography [32]

Figure 14. Degraded of Fig. 13 with σ=0.01

(a)

(b)

(c)

(d)

Figure 15. Brain tomography [32] a) Lee, SSIM: 0.9797 b) Wiener, SSIM: 0.9753 c) Conventional diffusion filter, SSIM: 0.9680 d) Proposed filter, SSIM: 0.9849

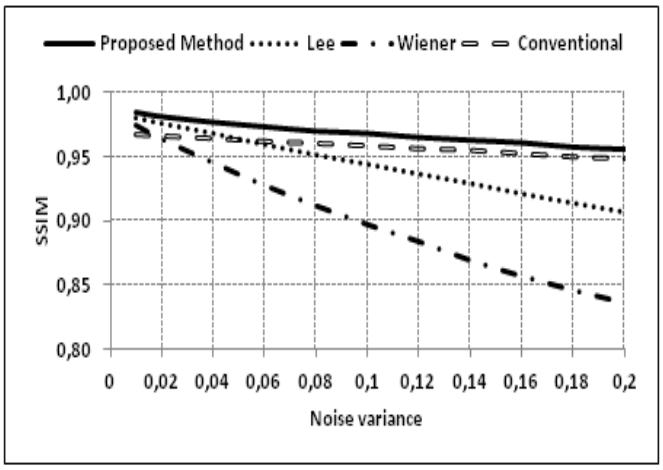

(a)

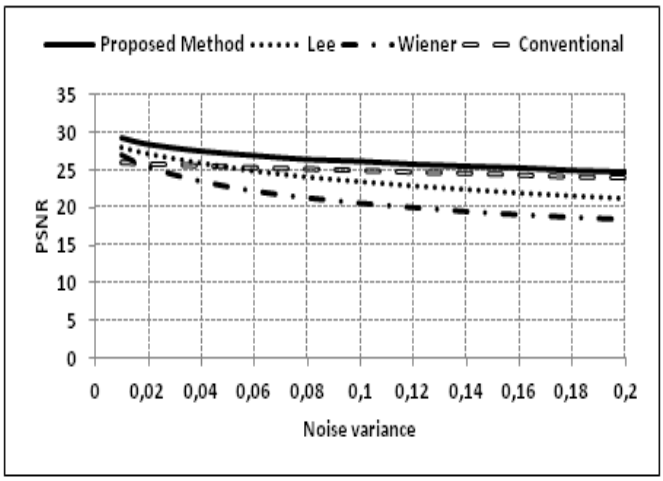

(b)

Figure 16. Performance curves with brain tomography a) SSIM versus variance b) PSNR versus noise variance

Wavelet-based anisotropic image filter developed was also tested with the real image shown in Fig. 13. It was firstly degraded with speckle noise as shown in Fig. 14, and then it was denoised with Lee and Wiener filter as illustrated in Fig. 15(a), and Fig. 15(b), respectively. Also, it was observed that the SSIM value of proposed filter was higher than that of the conventional anisotropic filter. Fig. 15(c) shows the output of conventional anisotropic filter whereas Fig. 15(d) shows the output of the proposed adaptive anisotropic filter.

Performance curves are given in Fig. 16(a), and Fig. 16(b). The filter of brain tomography also confirms that the wavelet-based anisotropic filter has resistance against to noises with different variances.

VII. CONCLUSIONS

In this study, a novel adaptive anisotropic diffusion filter without user intervention has been developed. The main filter parameter called, *K* is automatically calculated by the proposed method depending on noise variance in the image. Suggested method has been tested with different diffusivity functions, and it was verified that the most successful function was Weickert diffusivity function for image degraded by speckle noise. Performance of the developed anisotropic diffusion filter has been evaluated, and it was

indicated that the proposed method would be used for different images with speckle noises.

REFERENCES

[1] M. Petrou, C. Petrou, Image Processing: The Fundamentals, 2nd edn. Chichester, U.K.: Wiley, 2010, pp. 325. doi:10.1002/9781119994398

[2] H. Aghababaee, J. Amini, Y. C. Tzeng, "Improving change detection methods of SAR images using fractals," Sci Iranica, vol. 20, no. 1, pp. 15–22, 2013. doi:10.1016

[3] S. Saravani, R. Shad, M. Ghaemi, "Iterative adaptive Despeckling SAR image using anisotropic diffusion filter and Bayesian estimation denoising in wavelet domain," Multimedia Tools and Applications, vol. 77, no. 23, pp. 31469–31486, 2018. doi:10.1007/s11042-018-6153-8

[4] P. Perona, J. Malik, "Scale-space and edge detection using anisotropic diffusion," IEEE Trans. on Pattern Analysis and Machine Intelligence, vol. 12, no. 7, pp. 629-639, 1990. doi:10.1109/34.56205

[5] P. Charbonnier, L. Blanc-Feraud, G. Aubert, M. Barlaud, "Two deterministic half-quadratic regularization algorithms for computed imaging," in Proc. of ICIP-94, IEEE International Conference on Image Processing, vol. 2, pp. 168–172, 1994. doi:10.1109/ICIP.1994.413553

[6] J. Weickert, "Anisotropic diffusion in image processing," Teubner, Stuttgart, pp. 14-26, 1998.

[7] M. Black, G. Sapiro, D. H. Marimont, D. Heeger, "Robust anisotropic diffusion," IEEE Transactions on Image Processing, vol. 7, no. 3, pp. 421–432 , 1998. doi:10.1109/83.661192

[8] Y. Yu, S. T. Acton, "Speckle reducing anisotropic diffusion," IEEE Transactions on Image Processing. vol. 11, no. 11, pp. 1260-1270, 2002. doi:10.1109/TIP.2002.804276

[9] S. Aja, C. Alberola, J. Ruiz, "Fuzzy anisotropic diffusion for speckle filtering," Acoustics, Speech, and Signal Processing (ICASSP '01), vol. 2, pp. 1261-1264, 2001. doi:10.1109/ICASSP.2001.941154

[10] S. Gupta, R. C. Chauhan, S. C. Sexana, "Wavelet-based statistical approach for speckle reduction in medical ultrasound images," Medical and Biological Engineering and Computing, vol. 42, no. 2, pp. 189-192, 2004. doi:10.1007/BF02344630

[11] F. Maussang, J. Chanussot, S. C. Visan, M. Amate, "Adaptive anisotropic diffusion for speckle filtering in SAS imagery," Oceans 2005 Europe, vol. 1, pp. 305-309, 2005. doi:10.1109/OCEANSE.2005.1511730

[12] T. Joel, R. Sivakumar, "An extensive review on despeckling of medical ultrasound images using various transformation techniques," Applied Acoustics, vol. 138, pp. 18-27. doi:10.1016/j.apacoust.2018.03.023

[13] H. K. Rafsanjani, M. H. Sedaaghi, S. Saryazdi, "An adaptive diffusion coefficient selection for image denoising," Digital Signal Processing, vol. 64, pp. 71-82, 2017. doi:10.1016/j.dsp.2017.02.004

[14] S. Aja-Fernández, C. Alberola-López, "On the estimation of the coefficient of variation for anisotropic diffusion speckle filtering," IEEE Trans. on Image Processing, vol. 15, no. 9, pp. 2694-2701, 2006. doi:10.1109/TIP.2006.877360

[15] K. Krissian, C. F. Westin, R. Kikinis, K. G. Vosburgh, "Oriented speckle reducing anisotropic diffusion," IEEE Trans. on Image Processing, vol. 16, no. 5, pp. 1412-1424, 2007. doi:10.1109/TIP.2007.891803

[16] J. J. Nair, V. K. Govindan, "Speckle noise reduction using fourth order complex diffusion based homomorphic filter," In Advances in Computing and Information Technology, vol. 177, pp. 895-903, July 2012. doi: 10.1007/978-3-642-31552-7_91

[17] P. M. Shankar, "Use of phase diversity and modified phase congruence for edge enhancement in ultrasonic imaging," Signal, Image and Video Processing, vol. 7, no. 2, pp. 317-324, 2013. doi:10.1007/s11760-011-0240-x

[18] M. K. Alaoui, T. Nabil, M. Altanji, "On some new non-linear diffusion models for the image filtering. Applicable Analysis," vol. 93, no. 2, pp. 269-280, 2014. doi:10.1080/00036811.2013.769132

[19] R. Demirci, "Fuzzy adaptive anisotropic filter for medical images," Expert Systems, vol. 27, no. 3, pp. 219-229, 2010. doi:10.1111/j.1468-0394.2010.00525.x

[20] G. Singh, M. A. Ansari, "Efficient detection of brain tumor from MRIs using K-means segmentation and normalized histogram," In Information Processing (IICIP), 2016 1st India International Conference on, pp. 1-6, Aug. 2016.

[21] A. B. Spanier, N. Caplan, J. Sosna, B. Acar, L. Joskowicz, "A fully automatic end-to-end method for content-based image retrieval of CT scans with similar liver lesion annotations," International journal of computer assisted radiology and surgery, vol. 13, no. 1, pp. 165-174, 2018. doi:10.1007/s11548-017-1687-1

[22] P. Mercorelli, A. Frick, "Noise level estimation using haar wavelet packet trees for sensor robust outlier detection," In Computational Science and Its Applications-ICCSA, pp. 847-856, 2006. doi:10.1007/11751540_92

[23] S. Finn, M. Glavin, E. Jones, "Echocardiographic speckle reduction comparison," IEEE Trans. on Ultrasonics, Ferroelectrics and Frequency Control, vol. 58, no. 1, pp. 82-101, 2011. doi:10.1109/TUFFC.2011.1776

[24] R. Demirci, U. Tanyeri, "Anisotropic diffusion filter using Haar wavelet," In System Theory, Control and Computing (ICSTCC), pp. 1-6, Oct. 2012.

[25] D. L. Donoho, I. M. Johnstone, "Ideal spatial adaptation via wavelet shrinkage," Biometrika. vol. 81, no. 3, pp. 425–455, 1994. doi:10.1093/biomet/81.3.425

[26] G. Chang, B. Yu, M. Vetterli, "Adaptive wavelet thresholding for image denoising and compression," IEEE Trans. on Image Processing, vol. 9, no. 7, pp. 1352–1545, 2000. doi:10.1109/83.862633

[27] D. L. Donoho, "De-noising by soft-thresholding," IEEE Trans. on Inform. Theor., vol. 41, no. 3, pp. 613–627, 1995. doi:10.1109/18.382009

[28] G. Andria, F. Attivissimo, A. M. Lanzolla, M. A. Savino, "Suitable threshold for speckle reduction in ultrasound images," IEEE Trans. on Instrumentation and Measurement, vol. 62, no. 8, pp. 2270-2279, 2013. doi:10.1109/TIM.2013.2255978

[29] L. L. Huang, L. Xiao, Z. H. Wei, "Multiplicative noise removal via a novel variational model," EURASIP Journal on Image and Video Processing, vol. 2010, 2010. doi:10.1155/2010/250768

[30] J. Sun, Z. Xu, "Scale selection for anisotropic diffusion filter by Markov random field model," Pattern Recognition, vol. 43, no. 8, pp. 2630-2645, 2010. doi:10.1016/j.patcog.2010.02.019

[31] Z. Wang, A. C. Bovik, H. R. Sheikh, E. P. Simoncelli, "Image quality assessment: from error visibility to structural similarity," IEEE Trans. on Image Processing, vol. 13, no. 4, pp. 600-612, 2004. doi:10.1109/TIP.2003.819861

[32] R. C. Gonzalez, R. E. Woods, Digital image processing second edition, Prentice Hall, New Jersey, p. 59, 2002

[33] J. Lee, "Speckle analysis and smoothing of synthetic aperture radar images," Computer Graphics and Image Processing, vol. 17, pp. 24–32, 1981. doi:10.1016/S0146-664X(81)80005-6

[34] S. Solbo, T. Eltoft, "A stationary wavelet-domain wiener filter for correlated speckle," IEEE Trans. on Geoscience and Remote Sensing, vol. 46, no. 4, pp. 1219-1230, 2008. doi:10.1109/TGRS.2007.912718

[35] A. Ozcan, A. Bilenca, A. E. Desjardins, B. E. Bouma, G. J. Tearney, "Speckle reduction in optical coherence tomography images using digital filtering," Journal of the Optical Society of America A. vol. 24, no. 7, pp. 1901–1910, 2007. doi:10.1364/JOSAA.24.001901